PREPARATION AND CHARACTERIZATION OF CIPROFLOXACIN LOADED SILK FIBROIN AND GRAPHENE COMPOSITE ANTIBACTERIAL FILM

RAKESH MUTHA,[*,#] VISHAL SHRIRAO,[**] SOPAN NANGARE[***,#] and GANESH PATIL[****]

[*]*Department of Pharmacognosy, H. R. Patel Institute of Pharmaceutical Education and Research, Shirpur 425405, Maharashtra, India*
[**]*Department of Quality Assurance, H. R. Patel Institute of Pharmaceutical Education and Research, Shirpur 425405, Maharashtra, India*
[***]*Department of Pharmaceutics, Krishna Institute of Pharmacy, Krishna Vishwa Vidyapeeth (Deemed to be University), Karad 415539, Maharashtra, India*
[****]*Department of Quality Assurance, H. R. Patel Institute of Pharmaceutical Education and Research, Shirpur 425405, Maharashtra, India*
[#]*Authors contributed equally to this work*
✉ *Corresponding author: G. B. Patil, ganu16@gmail.com*

Received October 3, 2024

The present research work focuses on the development of ciprofloxacin hydrochloride (CF)-loaded silk fibroin (SF) and graphene (G) composite antibacterial films (CF@SF-G). In brief, the structural analysis, conducted using Fourier-transform infrared spectroscopy (FTIR), differential scanning calorimetry (DSC), X-ray diffraction (XRD), and scanning electron microscopy (SEM), revealed the incorporation of CF, SF, G, and glycerol. It ensured the formation of a silk II crystal structure with a β sheet conformation in all SF composite films. The composite films were fabricated by incorporating inorganic 'G' as a filler and glycerol as a plasticizer to enhance mechanical properties. A comprehensive characterization of the films was conducted, which included assessments of thickness, folding endurance, mechanical strength, swelling index, drug content, moisture content, moisture absorption, water vapor permeability, antibacterial activity, and *in vitro* drug release and permeation characteristics. Here, the results demonstrated that the addition of 'G' and glycerol to the CF@SF-G film (B-2) pointedly improved the mechanical properties of the SF composite films, as well as their moisture absorption, antibacterial activity, and *in vitro* release profile of CF, all of which are beneficial for wound healing. The B-2 sample exhibited superior elongation at break and flexibility compared to the pure SF films, which can be attributed to the reinforcing effects of 'G' and glycerol. Additionally, the B-2 composite films demonstrated good antibacterial activity, without compromising drug efficacy. In the future, such SF-based films can be used to reduce the risk of infection at the wound site and accelerate the wound healing process.

Keywords: silk fibroin, graphene, ciprofloxacin hydrochloride, antibacterial, composite film

INTRODUCTION

Burn injuries are a major global public health issue, contributing to considerable morbidity and mortality globally. Every year, over 180 million people are impacted by burn-related trauma, with roughly 11 million requiring serious medical treatment owing to the severity of their injuries. According to the World Health Organization (WHO) estimates for 2018, over 1 million people in India suffer moderate to severe burn injuries each year, putting a considerable strain on the country's healthcare system.[1,2] Burn injuries are frequently followed by substantial sequelae, such as functional impairments, extensive scarring, and contractures, which can severely limit the mobility and quality of life of those afflicted.[3] Burn wounds are extremely vulnerable to a wide spectrum of infections due to a variety of causes. Notably, the breakdown of the skin's protective barrier following a burn injury causes the production of protein-rich exudates, which create a perfect habitat for bacterial colonization and multiplication.[4-6] Infected burn wounds are a major

cause of postoperative complications, dramatically increasing the risk of sepsis and death. They account for almost one-quarter of all nosocomial infections, demonstrating their importance in patient outcomes and hospital-acquired morbidity.[7-9]

Gram-negative bacteria cause around 50% of burn wound infections. The most typically detected pathogens are *Staphylococcus aureus* (21 to 40% of infections) and *Pseudomonas aeruginosa* (6 to 15%). Other often involved micro-organisms include *Escherichia coli*, *Streptococcus pyogenes*, *Klebsiella pneumoniae*, and *Acinetobacter baumannii*, all of which are linked to pus production and serious consequences in burn site infections.[10-13] The increasing prevalence of drug-resistant strains, such as methicillin-resistant *S. aureus* (MRSA), complicates the management of burn wound infections and contributes to an increase in mortality among patients.[14] The use of sophisticated bio-interfaces and dressing materials with antibacterial and regenerative capabilities can aid in speeding up wound healing. These dressings keep the wound site wet, prevent dehydration, and permit gas and water vapor exchange, while staying impermeable to external pollutants like dust and bacteria. Furthermore, good wound dressings should be non-adhesive and easily detachable, reducing damage to healing tissue during dressing changes.[13,15,16]

Due to extraordinary properties, such as prominent biocompatibility, controllable biodegradability, high water and oxygen uptake, low immunogenicity, and tunable mechanical properties, silk fibroin (SF) based biomaterials from *Bombyx mori* (*B. mori*) have recently gained considerable attention in the scientific community. It has been widely reported for applications in the field of biomedicine, including tissue engineering, drug delivery, and wound healing.[17,18] In brief, SF is a main structural protein of silk fibers, accounting for 70-75% of total silkworm cocoons by weight.[19] The nature of SF being versatile, a variety of water-based processing therapeutic delivery systems with various dimensions and morphologies (*e.g*., films, gels, microparticles, nanoparticles,[20] tubes, sponges, composites, fibers) can be constructed by using numerous techniques.[19,21] Several studies have reported SF films as an outstanding substrate for propagation and adhesion of a range of cells (*e.g*., fibroblasts, osteoblasts, keratinocytes, epithelial, endothelial, and glial) for wound healing.[22,23] Previously, many studies have reported the modified release of therapeutic molecules from SF films.[24] Additionally, several research groups have prepared SF films reinforced with curcumin,[25,26] graphene oxide (GO) and reduced GO,[27] ciprofloxacin,[28] plant extract[29] and glycerol[30] for wound healing and biomedical applications. Pure SF films exhibit poor mechanical behavior, with stiffness, brittleness, and aqueous solubility, confining their applications. These characteristics of SF films could be potentially improved by the incorporation of a filler as a second phase and a plasticizer. Due to their remarkable mechanical properties, high binding potential, high aspect ratio, excellent flexibility, and superior processability, the most popular newfound fillers, graphene (G) and GO, have piqued the scientific community's interest in developing a range of composites applicable in the field of biomedicine.[31-33] Furthermore, the flexibility of SF films may be increased with the use of routinely used plasticizers, such as glycerol, to generate a more flexible system.[30]

In the present study, ciprofloxacin hydrochloride (CF), a broad-spectrum fluoroquinolone antibiotic, was selected as the model drug among various antibiotics to enhance the antibacterial and wound healing properties of SF films. CF is highly effective at very low concentrations and is commonly used to treat a wide range of bacterial infections due to its strong activity against both gram-positive and gram-negative pathogens. Additionally, it helps prevent airborne bacterial infections during the wound healing process.[28,34] Here, CF functions by inhibiting bacterial DNA gyrase, an enzyme essential for DNA replication and transcription in gram-negative bacteria and topoisomerase IV in gram-positive bacteria, which is crucial for resolving catenated DNA and relieving supercoiling during replication.[35] Owing to its broad-spectrum efficacy and low potential for resistance development, CF remains one of the most widely used antibiotics in wound healing applications.[34]

The present research aims to formulate CF@SF-G composite-based antibacterial films using a solution casting process, to augment mechanical properties and flexibility by incorporating varying amounts of ‘G’ as a filler and glycerol as a cross-linking agent. This study focuses on understanding the potential structural modifications in the SF film induced by the addition of ‘G’ and glycerol, evaluating the *in vitro* performance of the CF@SF-G composite films,

and ultimately developing an advanced CF@SF-G film as a promising biomaterial. In the future, the designed advanced composite film can be used for burn wound healing.

EXPERIMENTAL

Materials

Ciprofloxacin hydrochloride (CF) was generously provided by Glenmark Pharmaceuticals, Ltd. (Nashik, India). *Bombyx mori* (*B. mori*) silk cocoons were procured from Laxmi Sericulture Farming, Jalna, India. Graphene (G) was obtained from Asbury Carbons (New Jersey, USA). Lithium bromide (LiBr) was procured from Loba Chemie Private Ltd., India. Glycerol and sodium carbonate (Na_2CO_3) were obtained from Rankem Private Ltd., India. Mueller-Hinton Agar (MHA) was purchased from Loba Chemie Private Ltd., India. Sodium chloride (NaCl) was obtained from Rankem Private Ltd., India. The other reagents utilized in this work were of analytical grade.

Methods

Preparation of SF solution

The SF solution was prepared as per the formerly defined protocol.[19] Briefly, for one batch of SF, 5 *g* of *B. mori* silk cocoon pieces were degummed by adding to a 1 L boiling solution of 0.02 M Na_2CO_3 for 30 min. The degummed silk fibers were washed three times in distilled water for 20 min each to remove glue-like sericin before drying overnight at room temperature. The dried, degummed silk fibers were then dissolved in 9.3 M LiBr solution (20% w/v) for 4 h at 60 °C. The silk solution was then dialyzed against 1 L deionized water at room temperature (water was changed after 1, 3, 6, 24, 36, and 48 h) using a cellulose membrane (12kD MWCO), followed by centrifugation to remove undissolved materials at 9000 rpm for 15 min at 4 °C. Protein concentration was evaluated by drying a known volume of silk solution (6% w/v) for 12 h and quickly determining the mass of the residual solids.

Fabrication of CF@SF-G composite films

Ciprofloxacin hydrochloride (CF, 0.5 mg/mL) and 'G' were mixed with a 6% SF solution to prepare composite films. The 'G'-to-SF ratio was varied between 0.2, 0.4, 0.6, 0.8, and 1.0 weight percent (wt%) to obtain different formulations, as shown in Table 1. Glycerol (30 wt%) was used as a crosslinking agent to enhance film flexibility and stability. The preparation process involved vortexing the mixture for 5 min to achieve a homogeneous solution. The CF@SF-G composite films were then fabricated using the solvent casting method, where 14 mL of the prepared solution was poured onto 100 mm polystyrene petri dishes. The samples were incubated at 40 °C until fully dried, then carefully peeled off from the Petri dishes. The dried films were subsequently stored in a desiccator for further characterization.

Table 1
Various batches showing 'G' to SF proportion

Batch	SF conc. (wt%)	'G' conc. (wt%)	Glycerol conc. (wt%)	CF conc. (mg/mL)
SF	6.0	0.0	---	0.0
SF + glycerol	6.0	---	30	0.0
B-1	6.0	0.2	30	0.5
B-2	6.0	0.4	30	0.5
B-3	6.0	0.6	30	0.5
B-4	6.0	0.8	30	0.5
B-5	6.0	1.0	30	0.5

Characterization

Film thickness

The thickness of the pure SF film, SF-glycerol film, and CF@SF-G composite films, as dried in the Petri dishes, was determined by a digital Vernier caliper. The films were evaluated in three distinct regions (n = 3), and the mean (n = 3) was calculated.

Folding endurance

The folding endurances of the pure SF film, SF-glycerol film, and CF@SF-G film were measured to determine their flexibility, which is required for comfortable handling and secure wound application. It was determined by folding the film repeatedly (*n*) in the same place until the film broke. The value of the folding endurance was given by the number (*n*) of times the film could be folded at the same location without breaking.

Mechanical characteristics

Tensile strength

The tensile strengths of the pure SF films and the CF@SF-G composite films were tested using a CT3 texture analyzer (Brookfield Engineering Laboratories Inc., USA) with a load cell weighing 5 kg. Film strips 10 mm by 40 mm in size and free of air bubbles or imperfections were held between two clamps spaced 10 mm apart. The top clamp was used to pull the film at a speed of 0.5 mm/s. When the film broke, the tensile strength and percentage elongation were determined (*n* = 3).

Percent (%) elongation at break

The length of the exposed strip of the film's extensibility was determined by using a Vernier caliper until the strip broke. Equation (1) was used to calculate the % elongation at break:

$$\text{Elongation at break (\%)} = \frac{\text{final length} - \text{Initial length}}{\text{Initial length}} \times 100 \quad (1)$$

Swelling test

The swelling behavior of the CF@SF-G composite films was examined using the gravimetric technique. The dried, pre-weighed films were immersed in a pH 7.4 phosphate buffer solution. Swollen films (n = 3) were lifted and weighed every 24 h. The swelling index was determined using Equation (2):

$$\text{Swelling index} = \frac{\text{Wf} - \text{Wi}}{\text{Wi}} \times 100 \quad (2)$$

where Wi – initial weight of the dry film, and Wf – weight of the swollen film.

Drug loading

A pre-weighed sample (1 g) of each mechanically crushed CF@SF-G composite film (n = 3) was placed in a beaker containing 100 mL of pH 7.4 phosphate buffer solution. The beaker was covered with aluminum foil to protect the sample from photo-degradation and agitated on a magnetic stirrer at 100 rpm for 24 h to dissolve the drug. The solution was filtered using Whatman filter paper, and the concentration of the CF in the solution was determined spectrophotometrically at 276 nm (λmax) using Equation (3):

$$Drug\ loading\ (\%) = \frac{Total\ weight\ of\ film}{Amount\ of\ drug\ loaded} \times 100 \quad (3)$$

Percentage moisture content

The moisture content of the prepared CF@SF-G films (n = 3) was determined using the gravimetric method. Uniform film samples of 2 cm × 2 cm were carefully cut and weighed to record their initial weight (W_1) using an analytical balance. These samples (n = 3) were then placed in a hot air oven at 105 °C for 3 h to remove free moisture and subsequently reweighed to obtain the final weight (W_2). The moisture content (%) was calculated using Equation (4):

$$Moisture\ content\ (\%) = \frac{Initial\ weight\ (W_1) - Final\ weight\ (W_2)}{Initial\ weight\ (W_1)} \times 100 \quad (4)$$

Percentage moisture uptake

A pre-weighed sample (1 g) of each CF@SF-G composite film (n = 3) was placed in an incubator containing 200 mL of saturated solution of potassium chloride (KCl) (84% RH) at 25 °C. The films were removed, weighed, and the percent moisture uptake was determined using Equation (5):

$$\%\ Moisture\ uptake = \frac{Final\ weight - Initial\ weight}{Initial\ weight} \times 100 \quad (5)$$

Water vapor permeability

In 5 mL glass vials, 1 g of fused calcium chloride was placed, and a CF@SF-G composite film (n = 3) of 4 cm^2 was adhered to each vial opening with adhesive tape, so that the opening only had the composite film covering. The vials were weighed and kept in an incubator containing a saturated solution of potassium chloride (KCl, 84% RH) at 30 ºC for 24 h. The vials were detached, and the weight gain was recorded daily. The water vapor transmission rate (WVTR) of each CF@SF-G composite film was estimated using Equation (6):

$$WVTR\ (g/m^2/day) = \frac{Wf - Wi}{T \times A} \times 10^6 \quad (6)$$

where W_f – final weight (g), W_i – initial weight (g), T – time (days), A – surface area of the film (m^2) and 10^6 = conversion factor to express the result in g/m^2/day

Spectral analysis

An FTIR spectrophotometer (8400s) from Shimadzu Analytical India Pvt. Ltd. was used to examine the functional groups existing in the developed drug-loaded composites (CF@SF-G) in the range of 4000-400 cm^{-1}. The prepared films were cut into very small pieces and mixed with KBr (1:100), and finally, their FT-IR spectra were measured.

The DSC investigation is one of the fundamental methods to study how the physical properties of a sample change, along with temperature, over time. The thermal behavior of the CF@SF-G (B-2) composite films was studied by a DSC apparatus (STARe System DSC 1, Mettler Toledo Private Limited, USA). Samples weighing between 20 and 25 mg were wrapped in perforated aluminum pans and heated at a constant heating rate of 10 ºC/min at temperatures from 40 to 350 ℃.

Crystallinity and structural properties of the prepared films were determined using a D8 Advance X-ray diffractometer (Bruker AXS Analytical Instruments Private Limited, Germany) having a Cu Kα radiation beam operated at 40 kV and a current of 35 mA. The scans for XRD were performed over an angular range between 3 and 60º (2θ).

The surface morphology of the CF@SF-G composite films was imaged by using an SEM (JSM 6390LV, Japan Electron Optics Laboratory Limited, Japan) at an accelerating voltage of 20 kV. A briefly dried film sample of the required size was cut to prepare SEM specimens and mounted on the stub, using double-sided carbon tape, and the film surface was subjected to gold sputter coating, followed by scanning in the SEM.

In-vitro *drug release study*

In-vitro drug release studies were performed to determine the rate of release of CF from CF@SF-G composite films and the time required to release the total CF. The dialysis bag method was used to accomplish the CF release study from the CF@SF-G composite films. Films having a predetermined surface area of 4 cm^2

were placed in a beaker containing 100 mL of pH 7.4 phosphate buffer. The entire assembly was put on a magnetic stirrer set to 50 rpm at 32 °C. For analysis, aliquots of 5 mL were removed from the release medium at 1 h intervals up to 12 h and replaced with equivalent amounts of buffer solution to maintain steady conditions. The extent of CF released from each CF@SF-G composite film in the release medium was then measured spectrophotometrically at λmax of 276 nm.

In-vitro *drug permeation study*

In-vitro permeation measurement of CF@SF-G composite films was studied using a Franz diffusion assembly. Briefly, the CF@SF-G composite films were applied over the cellulose membrane mounted on the receptor compartment of the cell and fixed in place by affixing the donor compartment. The receptor compartment was filled with 15 mL of phosphate buffer having a pH of 7.4. The entire assembly was set over a magnetic stirrer at 37 °C. Aliquots of 3 mL were withdrawn at 1 h intervals from the diffusion cell for 12 h. An equal amount of fresh medium was introduced to the diffusion media, which assures a steady condition. The aliquots withdrawn were diluted ten times, and the concentration of the CF in the samples was measured spectrophotometrically at λmax of 276 nm.

Antimicrobial activity

The antibacterial activity of the pure SF film and the CF@SF-G composite film was assessed *in vitro* using the agar diffusion (zone of inhibition) method against the standard laboratory strain *Staphylococcus aureus* (*S. aureus*), a common Gram-positive pathogen associated with wound infections. In brief, MHA is a recommended medium for antibiotic susceptibility testing. Therefore, it was used to support bacterial growth. To prepare the medium, 3.8 g of MHA was dissolved in 100 mL of distilled water by heating with continuous stirring until completely dissolved, followed by sterilization in an autoclave at 121 °C for 15 min. After autoclaving, the medium was allowed to cool to approximately 45-50 °C, and poured aseptically into sterile Petri dishes to form a consistent 5 mm thick agar layer. The plates were left undisturbed to solidify and dry. Meanwhile, a fresh culture of *S. aureus* was grown overnight in nutrient broth and adjusted to a turbidity equivalent to 0.5 McFarland standard (approximately 1.5×10^8 CFU/mL). Under aseptic conditions, the bacterial suspension was evenly spread over the surface of MHA plates using a sterile cotton swab to ensure a uniform bacterial lawn. Sterile discs of pure SF and CF@SF-G films (each 1 cm² in size) were carefully placed on the inoculated plates using sterile forceps. A CF disc (5 µg) was included on each plate as a positive control to validate the antibacterial testing method. The prepared plates were then incubated in an upright position at 37 °C for 24 h. Following incubation, the antibacterial efficacy of the films was determined by measuring the diameter of the zones of inhibition formed around each film and the control disc using a Vernier caliper. Each experiment was performed in triplicate (n = 3) to ensure reproducibility, and the mean values of the inhibition zones were recorded and compared.

RESULTS AND DISCUSSION

Film thickness

The thicknesses of all prepared films, from pure SF to composite batches B-1 to B-5, are shown in Figure 1. Micrometer analysis revealed average thickness values ranging from 0.19 ± 0.08 mm (SF film) to 0.48 ± 0.08 mm (B-5). In the case of B-2, it was found to be 0.31 ± 0.06 mm. The increase in film thickness was attributed to the progressive incorporation of 'G' and other components that enhanced the film matrix density and structure.

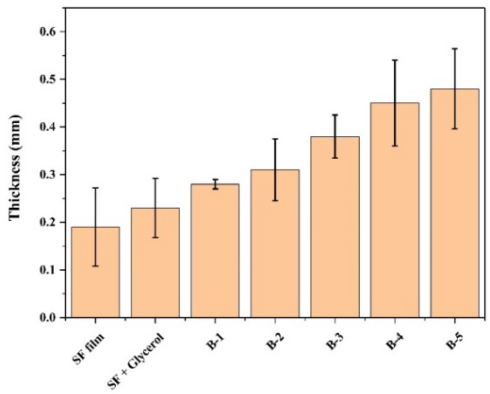

Figure 1: Thicknesses of the pure SF and the CF@SF-G composite films

Folding endurance

As summarized in Table 2, folding endurance progressively increased with the addition of glycerol and 'G'. The pure SF film exhibited the lowest endurance (49 ± 2 folds), whereas the SF + glycerol film showed the highest (78 ± 1 folds), highlighting glycerol's plasticizing effect. Among the composite films, Batch B-2 displayed the highest endurance (75 ± 2 folds), indicating an optimal balance between flexibility and structural reinforcement. Slight decreases in endurance in B-4 and B-5 were observed, likely due to brittleness induced by excess 'G'.

Table 2
Characterization summary of CF@SF-G composite films

Batch	Folding endurance	Swelling index (%)	Drug content (%)	Moisture content (%)	Moisture absorption (%)
SF film	49 ± 2	17.4 ± 0.6	---	9.5 ± 0.4	12.1 ± 0.5
SF + Glycerol	78 ± 1	20.3 ± 0.8	---	16.4 ± 0.5	27.6 ± 1.0
B-1	70 ±2	22.8 ± 0.9	72.4 ± 2.5	19.2 ± .0.5	36.2 ± 1.1
B-2	75 ± 2	31.5 ± 1.0	81.2 ± 2.1	23.8 ± 0.7	47.8 ± 1.5
B-3	73 ± 3	35.7 ± 1.2	84.6 ± 2.3	25.4 ± 0.8	49.1 ± 1.4
B-4	67 ± 2	39.8 ± 1.4	78.1 ± 2.0	27.1 ± 0.9	56.2 ± 1.8
B-5	63 ± 2	42.6 ± 1.5	76.8 ± 1.1	28.3 ± 0.8	60.4 ± 2.0

n = 3, ±: SD

Mechanical tests

Tensile strength

Figure 2 shows the tensile strength of the pure SF and CF@SF-G composite films. The tensile strength increased with the addition of glycerol and 'G'. The pure SF film showed the lowest strength (0.83 ± 0.04 MPa), while strength significantly improved in composite batches. Among them, B-3 exhibited the highest tensile strength (3.92 ± 0.12 MPa), followed by B-4 (3.56 ± 0.11 MPa) and B-2 (3.41 ± 0.10 MPa). This suggests that optimal 'G' concentrations enhance interfacial bonding and film integrity. At higher G loads (B-5), tensile strength slightly decreased (3.15 ± 0.09 MPa), likely due to 'G' agglomeration disrupting matrix homogeneity.[31]

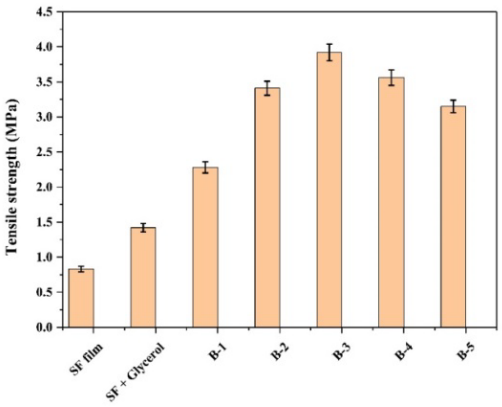

Figure 2: Tensile strength of pure SF film and CF@SF-G composite films

Percent elongation at break

As shown in Figure 3, elongation at break improved with the inclusion of glycerol and 'G'. The pure SF film was least flexible (16.2 ± 0.7%). In comparison, SF + glycerol improved it to 22.5 ± 0.8%, confirming glycerol's plasticizing effect. Composite batches showed a rising trend from B-1 (28.6 ± 0.9%) to a peak in B-2 (38.4 ± 1.2%), indicating optimal structural reinforcement. A slight decline in elongation was observed with higher 'G' content: B-3 (36.1 ± 1.1%), B-4 (34.7 ± 1.0%), and B-5 (31.5 ± 1.1%). These findings indicate B-2 as the best-balanced formulation for mechanical flexibility and stretchability.[31]

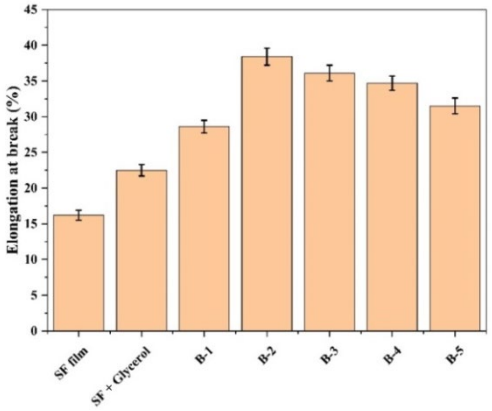

Figure 3: % Elongation at break analysis of pure SF film and CF@SF-G

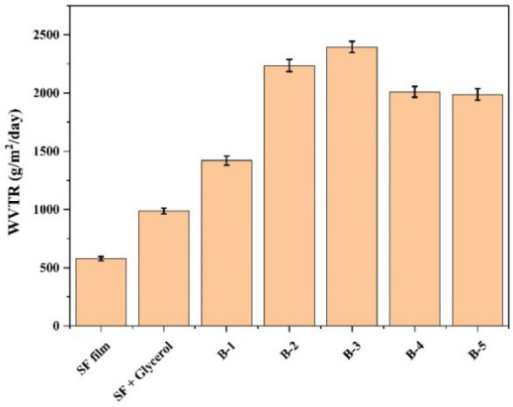

Figure 4: WVTR for the pure SF film, and all batches of CF@SF-G composite films

Swelling index

The swelling index values are presented in Table 2. The pure SF film had the lowest swelling index (17.4 ± 0.6%), while swelling increased with the addition of glycerol and 'G'. The highest value was recorded for B-5 (42.6 ± 1.5%), with B-3 close behind (35.7 ± 1.2%). Swelling increase reflects better hydrophilicity and porosity. However, further increases beyond B-3 led to marginal gains, possibly due to denser crosslinking that limited additional fluid uptake.

Percentage moisture content

Moisture content progressively increased from SF film (9.5 ± 0.4%) to B-5 (28.3 ± 0.8%). Glycerol contributed significantly to this upsurge (SF + glycerol: 16.4 ± 0.6%). Among composites, B-2 (23.8 ± 0.7%) and B-3 (25.4 ± 0.8%) had moderate moisture content, balancing flexibility and film integrity. Excess G (B-4 and B-5) led to higher retention, which may compromise storage stability.

Percentage moisture uptake

Moisture uptake followed a similar trend, with B-5 displaying the highest (60.4 ± 2.0%). Uptake increased from SF (12.1 ± 0.5%) and SF + glycerol (27.6 ± 1.0%) to a maximum in B-5. This increase reflects improved hydrophilicity, though excessive uptake may reduce barrier properties. B-2 (47.8 ± 1.5%) and B-3 (49.1 ± 1.4%) provided a good compromise between hydrophilicity and stability.

Water vapor transmission rate (WVTR)

In the case of wound dressing materials, WVTR is critical for moisture regulation. Pure SF had low WVTR (578 ± 18 g/m²/day), whereas B-2 (2236 ± 52 g/m²/day) and B-3 (2395 ± 48 g/m²/day) fell within the ideal wound healing range (2000-2500 g/m²/day). This suggests enhanced water vapor exchange from their optimized porous structures. Here, WVTR declined slightly in B-4 and B-5, which might be because of excessive compaction (Fig. 4).[36]

FTIR analysis

The FTIR spectra of CF (a), pure SF film (b), and B-2 composite films (c) are shown in Figure 5. From the FTIR spectra of the pure SF film and the B-2 composite films, it was observed that they exhibited identical absorption peaks with no shifts in the peaks, indicating no evidence of chemical interaction between the CF and the SF. Here, SF showed distinctive absorption bands in the range of 1700 to 1500 cm^{-1}, attributed to the peptide backbone of amide in SF. The peaks in the ranges of 1700-1600 cm^{-1}, 1600-1500 cm^{-1}, and 1266-1235 cm^{-1} were ascribed to amide I, amide II, and amide III, respectively.[31,32] As depicted in Figure 5 (b), the pure SF film exhibited peaks at positions 1670 cm^{-1} for amide I (C=O stretching), 1550 cm^{-1} for amide II (secondary N-H bending) attributed to silk I structure, and amide III (C-N stretching) at position 1246 cm^{-1}, attributed to the random coil and β sheet conformation, respectively. The B-2 composite films display similar peaks as observed in the pure SF film. Additionally, the peaks for CF at position 3375 cm^{-1} (O-H stretching), 2975 cm^{-1} (C-H stretching), 1740 cm^{-1} (C=O stretching), and 1317 cm^{-1} (C-F stretching) were observed in the FTIR spectrum of the B-2 composite films (Fig. 5c). The broadening of the peaks in the B-2 spectra resulted from the addition of the 'G'. The FTIR bands of amide I and amide II shifted from 1670 cm^{-1} to 1740 cm^{-1} and 1550 cm^{-1} to 1645 cm^{-1}, respectively, after the addition of 'G'. The results show that the silk II structure advances after the

incorporation of the 'G' into the B-2 composite films.[31]

Differential scanning calorimetry (DSC)

To understand any possible interactions between the CF and the SF, the DSC is extensively used. In brief, the thermal behaviors of all the samples are depicted in Figure 6. The thermogram of CF displays a large endothermic peak at 318 °C, which is ascribed to its melting transition. The peak observed in the range of 73 °C to 102 °C is probably related to the evaporation of bound water from both films. The thermograms of SF film and B-2 composite film also showed a strong peak between 240 °C-280 °C, which may be attributed to the thermal decomposition of the SF.[33]

X-ray diffraction (XRD)

In this step, XRD analysis was employed to understand the crystalline nature of the CF and the SF. The diffractograms of all the samples are depicted in Figure 7. In short, CF showed intense peaks at 8.17°, 9.01°, 19.26°, 26.39°, and 26.79° 2θ positions, which are attributed to the highly crystalline nature of CF.

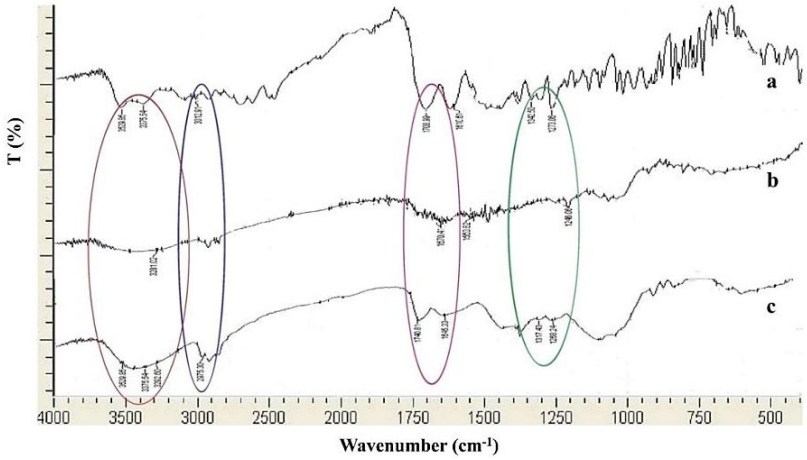

Figure 5: FTIR spectra of CF (a), pure SF film (b), and B-2 composite films (c)

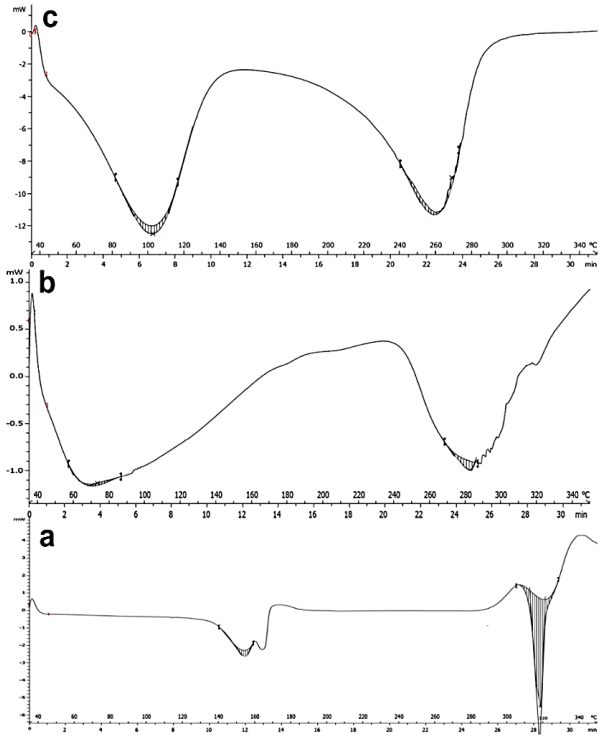

Figure 6: DSC thermograms of CF (a), pure SF (b), and B-2 composite films (c)

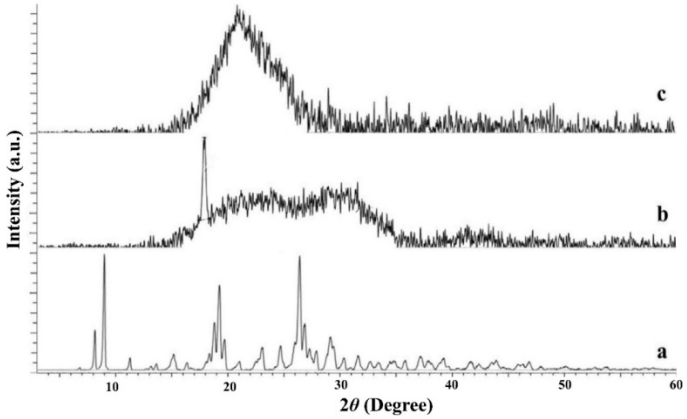

Figure 7: Diffractograms of CF (a), SF film (b), and B-2 composite films (c)

Furthermore, the diffractograms of pure SF film and B-2 composite films showed major dominant peaks at 17.88°, 31.35°, and 20.89° at the 2θ position, having d-spacings of 4.24, 2.85, and 4.96 Å, respectively, which are associated with the silk II structure. From the data obtained after XRD analysis, it was clear that pure CF is crystalline, whereas the SF and CF@SF-G films (B-2) were found to be amorphous.

Scanning electron microscopy (SEM)

The SEM micrograph in Figure 8 reveals the surface pattern and structure of the B-2 composite film. The exterior of the B-2 films has dominantly aggregated roughly scattered particle structures varying in size, as well as a moderate porosity level. The accumulation of 'G' increases the coarseness of the B-2 composite films, which might be due to the flaky and wrinkly nature of 'G'. The addition of 'G' in the B-2 films can contribute to increased roughness, which can advance cell adhesion, proliferation, and differentiation. Furthermore, the roughly distributed particle structures on the surface of the film designate that the surface can be appropriate for cell attachment.

Drug content

Drug content was highest in B-3 (84.6 ± 2.3%), followed by B-2 (81.2 ± 2.1%), indicating effective CF entrapment in these composite film batches. Lower drug content in B-1 (72.4 ± 2.5%), B-4 (78.1 ± 2.0%), and B-5 (76.8 ± 2.2%) suggests reduced loading efficiency at lower and higher G levels. The decline at higher 'G' levels might result from surface deposition or poor entrapment within compact matrices.

***In-vitro* drug release study**

Drug release after 12 h was highest in B-2 (98.2 ± 1.7%), followed by B-3 (96.9 ± 1.0%), likely due to optimal swelling behavior and higher porosity facilitating drug diffusion (Fig. 9). Batches B-1 (83.3 ± 1.7%), B-4 (80.8 ± 1.34%), and B-5 (95.9 ± 1.52%) exhibited comparatively lower drug release, potentially due to limited matrix relaxation or partial drug entrapment. These findings confirm that drug release is significantly influenced by the balance of 'G' content, matrix architecture, and swelling dynamics.

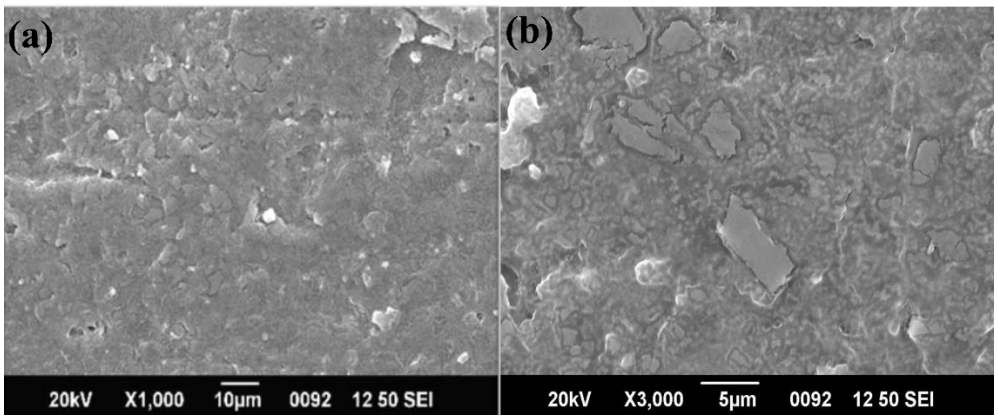

Figure 8: SEM images of the surface of B-2 composite film (a, b)

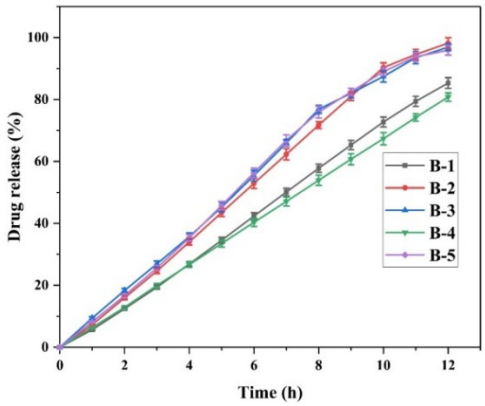

Figure 9: Comparative drug release profile from all SF composite films

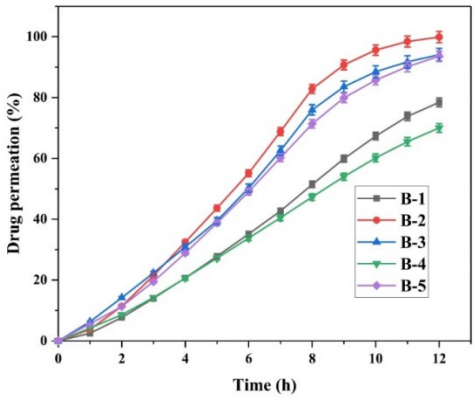

Figure 10: Comparative drug diffusion profile from all composite films

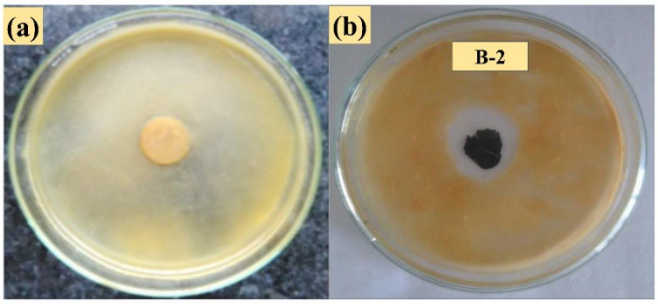

Figure 11: Antimicrobial activity of (a) pure SF film and (b) CF@SF-G film (B-2) against *S. aureus*

***In vitro* drug permeation study**

In vitro permeation data over 12 h are presented in Figure 10. In short, B-2 exhibited the highest drug permeation (99.87 ± 1.84%), even surpassing B-3. Although B-3 showed the highest drug release, its permeation was slightly lower (94.1 ± 2.08%), likely due to tighter matrix packing that may have restricted trans-membrane diffusion. Next, B-1 (78.45 ± 1.45%) and B-5 (93.56 ± 1.72%) demonstrated moderate permeation, while B-4 recorded the lowest value (70.03 ± 1.45%). Importantly, it may be due to over condensation of the matrix impeding drug mobility. These findings support B-2 as the most optimized formulation for achieving both modified release and effective transdermal permeation.

Antimicrobial susceptibility test

The antimicrobial zone of inhibition increased from 0 mm (SF and SF + glycerol) to 24.0 ± 1.0 mm (B-2) and 21.0 ± 0.9 mm (B-3), showing excellent antibacterial activity against *S. aureus* (Fig. 11). In brief, B-1 (18.0 ± 0.8 mm) had moderate efficacy. As well, B-4 and B-5 showed reduced zones (19.0 ± 0.9 mm and 17.0 ± 0.8 mm, respectively), likely due to drug diffusion limitations or 'G' aggregation. Here, B-2 was most effective, balancing dispersion and diffusion.

Considerations

The development of CF@SF-G composite films with varying concentrations of glycerol and 'G' was systematically optimized to enhance physicochemical, mechanical, and functional properties for potential wound-healing applications. The findings suggest that, while each compositional variation contributed differently to performance parameters, Batch B-2 consistently displayed the most balanced profile across critical benchmarks. Film thickness increased progressively with the addition of glycerol and 'G', indicating structural densification. The pure SF film had the lowest thickness, while B-5 peaked at high thickness, reflecting additive-induced matrix thickening. However, excessive thickness can hinder flexibility and permeability. The moderate thickness of B-2 demonstrated structural compactness without sacrificing handling properties.

Folding endurance was significantly enhanced by glycerol, which acted as a plasticizer, reducing intermolecular forces between polymer chains. The poor endurance of the pure SF film was amended substantially with glycerol alone. Composite films alike B-2 retained high durability, signifying an optimal balance between glycerol-induced flexibility and 'G'-mediated reinforcement. In contrast, higher 'G' levels (B-4 and B-5) introduced brittleness, and dropping endurance might be due to particle agglomeration and localized rigidity. Mechanical strength, decisive for functional integrity during application, peaked in B-3, signifying high 'G'-mediated reinforcement. However, B-2 provided appropriate strength with superior flexibility, as evinced by its highest elongation at break (%). This reflects ideal interfacial bonding and effective stress distribution across the polymer network. A marginal decline in elongation with increased 'G' content (B-4 and B-5) was likely due to rigid domain formation, which limits chain mobility.

Swelling index and moisture uptake both increased with higher 'G' and glycerol levels, indicating enhanced hydrophilicity. In this, B-5 exhibited good swelling and uptake, although excessive water retention may compromise barrier integrity and structural integrity under physiological conditions. Next, B-2 film's moderate swelling and uptake strike a desirable balance between maintaining moist wound conditions and ensuring mechanical stability. The drug content and release studies demonstrated that effective entrapment and sustained drug release were highly dependent on formulation composition. Moreover, B-2 exhibited good drug content and release, likely owing to its optimized porosity and matrix structure that facilitated diffusion. It accomplished good drug permeation, signifying a superior balance of film porosity and surface-area-to-volume ratio ideal for transdermal delivery. In contrast, B-1 and B-5 exhibited moderate to low performance, probably due to inefficient drug loading or entrapment within excessively compact or irregular matrices. Moisture content was found to upsurge with the inclusion of glycerol, reflecting its hygroscopic nature and possible role in modulating matrix flexibility and hydration. While high moisture content in B-5 may aid flexibility, it could also impair shelf stability. Moreover, B-2's content was adequate to guarantee flexibility without promoting microbial susceptibility or degradation during storage. WVTR data further supported the optimal characteristics of B-2 and B-3, falling within the ideal range for wound healing, thus ensuring adequate moisture evaporation without causing dehydration or exudate accumulation. As well, B-4 and B-5 displayed reduced WVTR due to denser packing, reducing diffusion channels.

Antimicrobial activity was significantly enhanced against *S. aureus* in composite batches, particularly B-2, telling unvarying dispersion of CF and 'G' in the matrix. Lower inhibition zones in B-4 and B-5 could be owing to particle aggregation, limiting diffusion or bioavailability of the antimicrobial agents.

Herein, FTIR, DSC, and XRD analyses confirmed the structural integrity of the drug-polymer system. As well, FTIR revealed no major chemical interactions, while shifts in amide bands indicated the development of the silk II crystalline structure. Moreover, DSC analysis confirmed thermal compatibility and successful CF incorporation, with B-2 showing thermal peaks consistent with both SF and CF. As well, XRD showed that pure CF was crystalline, whereas SF and B-2 were more amorphous, improving drug loading and release characteristics. In addition, SEM micrographs of B-2 revealed moderately rough, porous surfaces due to 'G' wrinkled morphology. These topographical features are advantageous for cellular interactions, including adhesion and proliferation, making B-2 particularly favorable for biomedical applications like wound dressings or transdermal patches. The cumulative data emphasize that B-2 exhibits an optimal combination of mechanical strength, flexibility, drug delivery efficiency, antimicrobial efficacy, and structural integrity. The carefully modulated 'G' and glycerol content in B-2 results in a balanced film matrix that fulfils crucial functional standards for a biomedical film, especially for wound healing applications. Future detailed investigations involving *in vivo* testing and biocompatibility studies are warranted to further establish its clinical utility.

CONCLUSION

In this research work, antibacterial CF@SF-G composite films were successfully fabricated using CF, SF, and 'G'. In brief, SF acted as a biopolymeric matrix, CF served as the antibacterial agent, and the incorporation of 'G' and glycerol enhanced both mechanical and functional attributes of the films. FTIR analysis confirmed the molecular integrity of CF within the SF matrix, while both FTIR and XRD results demonstrated an

increase in β-sheet content, suggesting improved crystallinity and structural stability upon incorporation of 'G' and glycerol. Mechanical evaluation revealed a trade-off between tensile strength and flexibility: although tensile strength declined with higher 'G' concentrations, elongation at break and folding endurance improved significantly owing to the synergistic effect of structural reinforcement by 'G' and plasticization by glycerol. All composite films exhibited desirable moisture content, fluid uptake capacity, and WVTR, parameters critical for maintaining a moist wound environment conducive to healing. Importantly, SEM analysis showed a rough, flaky surface morphology, attributed to 'G' addition, which could facilitate cell attachment and proliferation. Among all formulations, Batch B-2 emerged as the optimal candidate, demonstrating a balanced profile of mechanical integrity, WVTR, and customized CF release, achieving good CF permeation over 10 h without burst release. Moreover, it showed good antibacterial potential against *S. aureus*, which might be due to the combined effect of CF, G, and SF in the composite matrix. Overall, the optimized B-2 film offers a promising biomaterial for wound dressing, particularly in managing burns and chronic wounds, by delivering sustained antibacterial action along with favorable mechanical, physicochemical, and morphological properties that support effective wound healing.

REFERENCES

[1] K. Jyoti, G. Malik, M. Chaudhary, M. Sharma, M. Goswami *et al*., *Int. J. Biol. Macromol*., **161**, 325 (2020), https://doi.org/10.1016/j.ijbiomac.2020.05.230

[2] M. Abazari, A. Ghaffari, H. Rashidzadeh, S. Momeni Badeleh and Y. Maleki, *J. Biomed. Mater. Res. B Appl. Biomater*., **108**, 1934 (2020), https://doi.org/10.1002/jbm.b.34535

[3] M. D. Peck, *Burns*, **37**, 1087 (2011), https://doi.org/10.1016/j.burns.2011.06.005.

[4] J. L. Soares de Macedo and J. B. Santos, *Burns*, **32**, 477 (2006), https://doi.org/10.1016/j.burns.2005.11.012

[5] R. B. Ahuja, A. Gupta and R. Gur, *Burns*, **35**, 672 (2009), https://doi.org/10.1016/j.burns.2008.08.015

[6] D. Church, S. Elsayed, O. Reid, B. Winston, R. Lindsay *et al*., *Clin. Microbiol. Rev*., **19**, 403 (2006), https://doi.org/10.1128/CMR.19.2.403-434.2006

[7] R. W. Haley, D. H. Culver, J. W. White, W. M. Morgan and T. G. Emori, *Am. J. Epidemiol*., **121**, 159 (1985), https://doi.org/10.1093/oxfordjournals.aje.a113988

[8] R. L. Nichols, *Emerg. Infect. Dis*., **7**, 220 (2001), https://doi.org/10.3201/eid0702.010214

[9] A. J. Singer and S. A. McClain, *Wound Repair Regen*., **10**, 372 (2002), https://doi.org/10.1046/j.1524-475x.2002.10606.x

[10] T. Sewunet, Y. Demissie, A. Mihret and T. Abebe, *Ethiop. J. Health Sci*., **23**, 209 (2013), https://doi.org/10.4314/ejhs.v23i3.3

[11] J. C. Lawrence, *Burns*, **18**, S23 (1992), https://doi.org/10.1016/0305-4179(92)90066-4

[12] P. M. Kumar and A. Ghosh, *Eur. J. Pharm. Sci*., **96**, 243 (2017), https://doi.org/10.1016/j.ejps.2016.09.038

[13] A. Yerra and D. M. Mamatha, *Polym. Adv. Technol*., **32**, 861 (2021), https://doi.org/10.1002/pat.5137

[14] S. Tajik, S. Najar-Peerayeh, B. Bakhshi and R. Golmohammadi, *Iran. J. Pathol*., **14**, 284 (2019), https://doi.org/10.30699/ijp.2019.94189.1917

[15] R. Jayakumar, M. Prabaharan, P. T. Sudheesh Kumar, S. V. Nair and H. Tamura, *Biotechnol. Adv*., **29**, 322 (2011), https://doi.org/10.1016/j.biotechadv.2011.01.005

[16] A. Vasconcelos, A. C. Gomes and A. Cavaco-Paulo, *Acta Biomater*., **8**, 3049 (2012), https://doi.org/10.1016/j.actbio.2012.04.035

[17] E. Wenk, H. P. Merkle and L. Meinel, *J. Control Release*, **150**, 128 (2011), https://doi.org/10.1016/j.jconrel.2010.11.007

[18] M. Farokhi, F. Mottaghitalab, Y. Fatahi, A. Khademhosseini and D. L. Kaplan, *Trends Biotechnol*., **36**, 907 (2018), https://doi.org/10.1016/j.tibtech.2018.04.004

[19] D. N. Rockwood, R. C. Preda, T. Yücel, X. Wang, M. L. Lovett *et al*., *Nat. Protoc*., **6**, 1612 (2011), https://doi.org/10.1038/nprot.2011.379

[20] H. Rahmani, A. Fattahi, K. Sadrjavadi, S. Khaledian, Y. Shokoohinia *et al*., *Adv. Pharm. Bull*., **9**, 601 (2019), https://doi.org/10.15171/apb.2019.069

[21] M. A. Tomeh, R. Hadianamrei and X. Zhao, *Pharmaceutics*, **11**, 494 (2019), https://doi.org/10.3390/pharmaceutics11100494

[22] T. L. Liu, J. C. Miao, W. H. Sheng, Y. F. Xie, Q. Huang *et al*., *J. Zhejiang Univ. Sci. B*., **11**, 10 (2010), https://doi.org/10.1631/jzus.B0900163

[23] W. Zhang, L. Chen, J. Chen, L. Wang, X. Gui *et al*., *Adv. Healthc. Mater*., **6** (2017), https://doi.org/10.1002/adhm.201700121

[24] Y. Huang, K. Bailey, S. Wang and X. Feng, *React. Funct. Polym*., **116**, 57 (2017), https://doi.org/10.1016/j.reactfunctpolym.2017.05.007

[25] N. Kasoju and U. Bora, *J. Biomed. Mater. Res. B Appl. Biomater*., **100**, 1854 (2012), https://doi.org/10.1002/jbm.b.32753

[26] Z. Karahaliloglu, *Mater. Tech*., **33**, 276 (2018), https://doi.org/10.1080/10667857.2018.1432171

[27] S. Aznar-Cervantes, J. G. Martínez, A. Bernabeu-Esclapez, A. A. Lozano-Pérez, L. Meseguer-Olmo *et al*., *Bioelectrochemistry*, **108**, 36 (2016), https://doi.org/10.1016/j.bioelechem.2015.12.003

[28] A. K. M. M. Alam and Q. T. H. Shubhra, *J. Mater. Chem. B*., **3**, 6473 (2015), https://doi.org/10.1039/C5TB00920K

[29] G. Basal, D. Altıok and O. Bayraktar, *Fibers Polym*., **11**, 21 (2010), https://doi.org/10.1007/s12221-010-0021-0
[30] L. Xiufang, Z. Huijie, H. Lei, C. Zhen, T. Ziq *et al*., *Compos*. *B Eng*., **152**, 305 (2018), https://doi.org/10.1016/j.compositesb.2018.08.136
[31] N. I. S. M. Yusoff, M. U. Wahit, J. Jaafar and T. W. Wong, *Today Proc*., **5**, 21853 (2018), https://doi.org/10.1016/j.matpr.2018.07.042
[32] L. Wang, C. Lu, B. Zhang, B. Zhao, F. Wu *et al*., *RSC Adv*., **4**, 40312 (2014), https://doi.org/10.1039/C4RA04529G
[33] Y. Yang, X. Ding, T. Zou, G. Peng, H. Liu *et al*., *RSC Adv*., **7**, 7954 (2017), https://doi.org/10.1039/C6RA26807B
[34] E. Okoye and T. Okolie, *Int. J. Health Allied Sci*., **4**, 234 (2015), https://doi.org/10.4103/2278-344X.167660
[35] M. Contardi, J. A. Heredia-Guerrero, G. Perotto, P. Valentini, P. P. Pompa, *et al*., *Eur. J. Pharm. Sci*., **104**, 133 (2017), https://doi.org/10.1016/j.ejps.2017.03.044
[36] M. L. Cacicedo, G. Pacheco, G. A. Islan, V. A. Alvarez, H. S. Barud *et al*., *Int. J. Biol. Macromol*., **147**, 1136 (2020), https://doi.org/10.1016/j.ijbiomac.2019.10.082